IEEE Access
Multidisciplinary | Rapid Review | Open Access Journal

Received January 5, 2020, accepted January 14, 2020, date of publication January 17, 2020, date of current version January 28, 2020.

Digital Object Identifier 10.1109/ACCESS.2020.2967409

Experimental Demonstration of DFT-Precoded Guard-Band OSSB-OFDM Signal Reception With ADC Undersampling Technique

MING CHEN[1], (Member, IEEE), LONG ZHANG[1], DONGSHENG XI[1], GANG LIU[1], HUI ZHOU[2], AND QINGHUI CHEN[3]

[1]School of Physics and Electronics, Hunan Normal University, Changsha 410081, China
[2]College of Information Science and Engineering, Hunan Normal University, Changsha 410081, China
[3]College of Computer and Communication, Hunan University of Technology, Zhuzhou 412007, China

Corresponding author: Ming Chen (ming.chen@hunnu.edu.cn)

This work was supported in part by the National Natural Science Foundation of China under Grant 61805079 and Grant 61701180, and in part by the Scientific Research Fund of Hunan Provincial Education Department under Grant 18B026, Grant 17C0957, and Grant 18C0520.

ABSTRACT Guard-band optical single-side-band orthogonal frequency-division multiplexing (GB-OSSB-OFDM) is a good solution to achieve long-haul transmission as well as high receiver sensitivity. A low-complexity receiver with ADC undersampling technique is experimentally demonstrated in a GB-OSSB-OFDM transmission system. The principle of the proposed ADC undersampling technique and the constraint conditions on the use of such a technique are presented and discussed in detail. Besides, the discrete Fourier transform (DFT) precoding technique is also applied to reduce the peak-to-average power ratio (PAPR) of the baseband GB-OFDM signal as well as improve bit error rate (BER) performance. By using the DFT precoding technique, it exhibits that the PAPR of the GB-OFDM signal can be reduced by about 6 dB at the complementary cumulative distribution function (CCDF) of 1×10^{-3}. After 100 km standard single-mode fiber (SSMF) transmission, the results show that the ADC undersampled low-complexity receiver has similar BER performance with the conventional oversampled GB-OFDM receiver. At the BER of 3.8×10^{-3}, the receiver sensitivity in terms of received optical power can be improved by about 2 dB with the DFT precoding technique.

INDEX TERMS Guard-band orthogonal frequency-division multiplexing (GB-OFDM), undersampling technique, optical single-sideband (OSSB), discrete Fourier transform (DFT) precoding.

I. INTRODUCTION

Nowadays, with the development of 5G mobile networks, Internet of thing networks and clouding computing, etc., which are driving the data rate up to 400 Gbit/s and beyond in data centers [1]–[3]. In access networks, the 40-Gigabit-capable passive optical network (PON) known as next-generation PON stage 2 (NG-PON2) has been discussed and standardized in the ITU-T Recommendation G. 989 series [4]. The transmission distance is increased up to 40 km. To meet the ever-increasing capacity and transmission distance requirement for future generation long-reach PON systems, it is interesting to investigate advanced physical-layer technologies to support the requirements with low-cost. Optical orthogonal frequency-division multiplexing (OFDM) has been regarded as a promising technology for long-reach and high-speed optical communication systems, due to its high spectral efficiency (SE), robustness to optical fiber dispersions and powerful digital signal processing (DSP) techniques [5]–[7]. OFDM based PON systems have been proposed and experimentally demonstrated with both direct detection [7], [8] and coherent detection [9], [10]. In coherent detection, several sophisticated optical and electrical devices, as well as complex DSP algorithms, are required. It increases system cost and power consumption. In contrast, direct-detection optical OFDM (DDO-OFDM) has a simple structure and can be implemented at low cost and power consumption. However, there exist two major problems of low receiver sensitivity and power fading induced by chromatic dispersion (CD) in DDO-OFDM systems.

The associate editor coordinating the review of this manuscript and approving it for publication was Tianhua Xu.

Optical single-side-band (OSSB) modulation is an efficient method to combat CD-induced power fading and has been widely used in DDO-OFDM [11]–[16]. However, how to improve the receiver sensitivity of DDO-OFDM efficiently is still an open question. High optical carrier-to-signal power ratio (CSPR) is the main reason for the low receiver sensitivity. The received signal will be interfered with by the subcarrier-to-subcarrier beating interference (SSBI) at the photodiode if the CSPR is reduced. As a result, the receiver performance may be deteriorated. In the literature, there are mainly three types of methods to avoid or compensate SSBI and then improve the receiver sensitivity. The first one is the use of a guard band to prevent data subcarriers from SSBI [12], [13]; the second one is balanced detection with dual photodiodes to cancel SSBI [14], [15]; the third one is with the help of advanced DSP algorithms to compensate SSBI [16], [17]. The guard-band (GB) method can operate at an optimal CSPR of 0 dB, but reduces SE; while the complex balanced receiver is required for the method of balanced detection and increases the hardware complexity. The DSP-aided method has high SE and low hardware complexity; however, the optimal CSPR is larger than that of the GB method, due to the residual SSBI. Recently, a spectrally-efficient guard band twin-SSB technique is proposed and experimentally demonstrated [18]. The data rate is doubled in comparison with the conventional GB OSSB-OFDM. In our previous work [19], it showed that the receiver sensitivity can be improved by using an optical IQ modulator. The optimal CSPR is still around 0 dB. Therefore, the GB method may be a good option to achieve high receiver sensitivity of OSSB-OFDM.

In both the conventional GB OSSB-OFDM and twin-SSB-OFDM receivers [12], [13], [18], the baseband GB-OFDM signals are usually oversampled by a high-speed ADC with a sampling rate of greater than four times its bandwidth. However, the oversampling inevitably increases the ADC output data rate, power consumption, and ADC cost. Meanwhile, the power and cost of the receiver DSP chips such as field programmable gate array (FPGA) increase as it has to capture high-speed data. From the perspective of real applications, it is not an efficient way to implement the GB-OFDM receivers. One possible solution with low-complexity implementation is to reduce ADC sampling rate. In [20], a low sampling rate (LSR) receiving scheme with digital preprocess was proposed for a 100-GHz OFDM-based radio-over-fiber (OFDM-RoF) system with direct detection. Besides, a simplified aliasing-based sub-Nyquist sampling technique with post-processing was also proposed and experimentally demonstrated in 128×128 multiple-input multiple-output (MIMO) OFDM system with LSR ADC arrays for mobile fronthaul [21]. Moreover, pre-processing-based sub-Nyquist sampling with channel-characteristic-division multiplexing (CCDM) [22] or delay-division multiplexing (DDM) [23], [24] schemes are also proposed and verified in OFDM-PON. To achieve a low sampling rate, these schemes require complex pre- or/and post-processing. In addition, channel characteristics and accurate delays are also required for CCDM and DDM schemes, respectively. In our previous work [25], we have proposed a simple ADC undersampling technique with reduced DSP algorithms for GB-OFDM receivers. This technique allows the use of ADC with a low sampling rate as well as reduces the hardware implementation of the DSP algorithms such as timing synchronization and DFT operation. However, the proposed ADC undersampling technique was only studied by numerical simulations. It is interesting to experimentally investigate this technique in a GB-OSSB-OFDM system to fully verify its performance. Besides, the high peak-to-average power ratio (PAPR) is still a problem for these OSSB-GB-OFDM transmission systems. DFT precoding (also known as DFT-spread) is a powerful DSP method to reduce the PAPR and, in the meantime, balance the signal-to-noise ratio (SNR) among the data-carrying subcarriers and then improve bit error rate (BER) performance. It has been extensively studied in optical OFDM systems [26], [27].

In this work, we present the principle of the proposed ADC undersampling technique in detail and discuss the constraint conditions on the use of such a technique. DFT precoding technique is applied to reduce PAPR of the baseband GB-OFDM signal as well as improve the BER performance. The PAPR of the precoded GB-OFDM signal is investigated by numerical simulation. Subsequently, the DFT-precoded GB-OSSB-OFDM signals over 100 km standard single-mode fiber (SSMF) transmission with the proposed ADC undersampling technique is experimentally demonstrated for the first time.

The rest of this paper is organized as follows. Section II presents the operation principle of the ADC undersampling technique in detail and discusses the constraint conditions on the use of such a technique. The principle of DFT precoding and decoding is described in Section III. Experimental setup is described in Section IV. Simulated and experimental results are provided and discussed in Section V. Conclusions are drawn in Section VI.

II. OPERATION PRINCIPLE AND CONSTRAINT CONDITIONS

The block diagram of the operating principle of the ADC undersampling technique is illustrated in Fig. 1. In the receiver, the spectrum of the recovered GB-OFDM signal after optical-to-electrical conversion (OEC) is shown in Fig. 1(a). The guard band has the same bandwidth (B) as the signal. And the GB is filled with SSBI after OEC. The baseband GB-OFDM signal is first filtered with a band-pass filter with a bandwidth of B to suppress the SSBI before performing the analog-to-digital conversion. In the literature, the filtered GB-OFDM signal is often oversampled at a sampling rate of greater than $4B$ samples per second (Sa/s). For the proposed technique, the signal is undersampled at $2B$ Sa/s. It should be pointed out that the requirement on the bandwidth of ADC should be still more than $2B$ Hz rather than B Hz for the ADC undersampling technique.

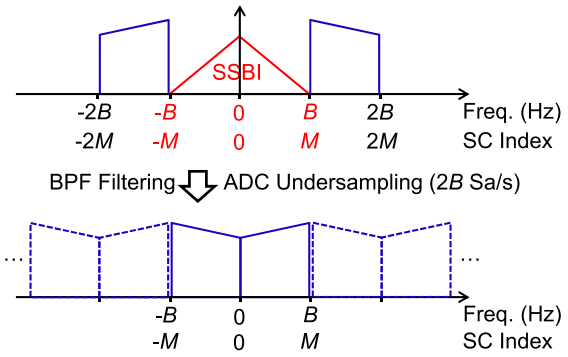

FIGURE 1. Block diagram of the operating principle of the proposed ADC undersampling technique.

In the GB-OFDM transmitter, we assume that the inverse DFT (IDFT) size is N and DAC sampling rate is R_{DAC}. The length of the cyclic prefix (CP) is N_{CP}. Direct current (DC) subcarrier is reserved for DC bias and M subcarriers in the low-frequency bins are filled with zeros for the GB. M subcarriers with indices from $M+1$ to $2M$ are used to carry data. The input vector of N-point IDFT is constrained to have Hermitian symmetry (HS). The sampling rate of ADC (R_{ADC}) should be $2B$ Sa/s and the relationship between R_{ADC} and R_{DAC} is given by

$$R_{\mathrm{ADC}} = \frac{2M}{N} R_{\mathrm{DAC}} \tag{1}$$

Once ADC undersampling is done, the DFT size in the receiver DSP is reduced to $2M$. Similarly, the length of CP will also be shorted. Here, we define its length as N_{CPR}. The N_{CPR} has a relationship with N_{CP} as follow

$$N_{\mathrm{CPR}} = \frac{2M}{N} N_{\mathrm{CP}} \tag{2}$$

The value of N_{CP} should be constrained so that N_{CPR} can be a non-negative integer number.

We define the i-th subcarrier modulated with frequency-domain data a_i in the GB-OFDM transmitter, where i ranges from $M+1$ to $2M$ and $-2M$ to $-M-1$. The input vector of N-point IDFT has been constrained to have HS, i.e., $a_i = a^*_{-i}$. In the receiver, the recovered data after $2M$-point DFT on the i-th subcarrier is b_k and the range of k is from $-M+1$ to M, where $b_k = b_{-k^*}$. As we can see from Fig. 1, the subcarrier index of the recovered data after the ADC undersampling operation has changed. The relationship between b_k and a_i can be expressed as

$$b_k = \begin{cases} H_{k+2M} \cdot a_{k+2M} + w_k, & k \in [-M+1, -1] \\ H_{-2M} \cdot a_{-2M} + H_{2M} \cdot a_{2M} + w_k, & k = 0 \\ H_{k-2M} \cdot a_{k-2M} + w_k, & k \in [1, M-1] \\ w_k, & k = M \end{cases} \tag{3}$$

where H_i is the channel response on the i-th subcarrier before undersampling, and $H_i = H^*_{-i}$. w_k presents the noise on the k-th subcarrier of the undersampled signal. From Eq. (3), we can observe that there two special cases: $k = 0$ and $k = M$. The image part of the data on the DC subcarrier ($k = 0$) will be canceled due to the superposition of two conjugate data a_{-2M} and a_{2M} carried on the $\pm 2M$-th subcarriers before ADC undersampling. Generally, these two subcarriers should be modulated with amplitude modulation formats in the transmitter. However, the real part of the data on the DC subcarrier after undersampling is significantly attenuated if the phase response on the $\pm 2M$-th subcarrier approaches or equals to $\pm\pi/2$ before undersampling. In this case, $b_0 \rightarrow w_0$, so it is difficult to recover the data on the DC subcarrier after undersampling. One possible solution is to multiply the two subcarriers by an anti-phase factor in the transmitter if the channel phase response is stable. Otherwise, these two subcarriers should be reserved and filled with zeros. Besides, the M-th subcarrier after undersampling does not carry data.

The benefits from the use of the proposed ADC undersampling technique for the GB-OFDM receiver are twofold. Firstly, the sampling rate of ADC can be halved. It will relax the design of high-speed ADC and reduce its cost and power consumption. Secondly, the operating clock frequency or on-chip resource usage of FPGA/ASICs chips for hardware implementation can be reduced due to the reduction of sample rate and DFT size.

III. DFT PRECODING AND DECODING

In the transmitter, the pseudo-random binary sequence (PRBS) is first mapped to M complex-valued QAM symbols (a_m, $m \epsilon [0, M-1]$) for each GB-OFDM symbol generation. For the DFT precoding, the precoded symbols can be expressed as

$$[d_0, d_1, \ldots, d_{M-1}] = [a_0, a_1, \ldots, a_{M-1}]\, W_{M\times M} \tag{4}$$

where $W_{M\times M}$ is the DFT matrix with a size of $M \times M$, and it is given by

$$W_{M\times M} = \frac{1}{\sqrt{M}} \begin{bmatrix} 1 & 1 & 1 & \cdots & 1 \\ 1 & w & w^2 & \cdots & w^{M-1} \\ \vdots & \vdots & & & \\ 1 & w^{M-1} & w^{2(M-1)} & \cdots & w^{(M-1)(M-1)} \end{bmatrix} \tag{5}$$

where $w = e^{-\mathrm{j}2\pi/N}$ in which $j^2 = -1$. In the receiver, the channel equalized signal $\left[\hat{d}_0, \hat{d}_1, \ldots, \hat{d}_{M-1}\right]$ is decoded with DFT inverse matrix $W^{-1}_{M\times M}$ as follow

$$[\hat{a}_0, \hat{a}_1, \ldots, \hat{a}_{M-1}] = \left[\hat{d}_0, \hat{d}_1, \ldots, \hat{d}_{M-1}\right] W^{-1}_{M\times M} \tag{6}$$

IV. EXPERIMENTAL SETUP

A proof-of-concept experimental setup of the GB-OSSB-OFDM system with direct detection for long-reach applications is established as shown in Fig. 2. In the transmitter DSP, a PRBS with a period length of $2^{20}-1$ is generated for 16-QAM symbol mapping. Two random binary sequences are

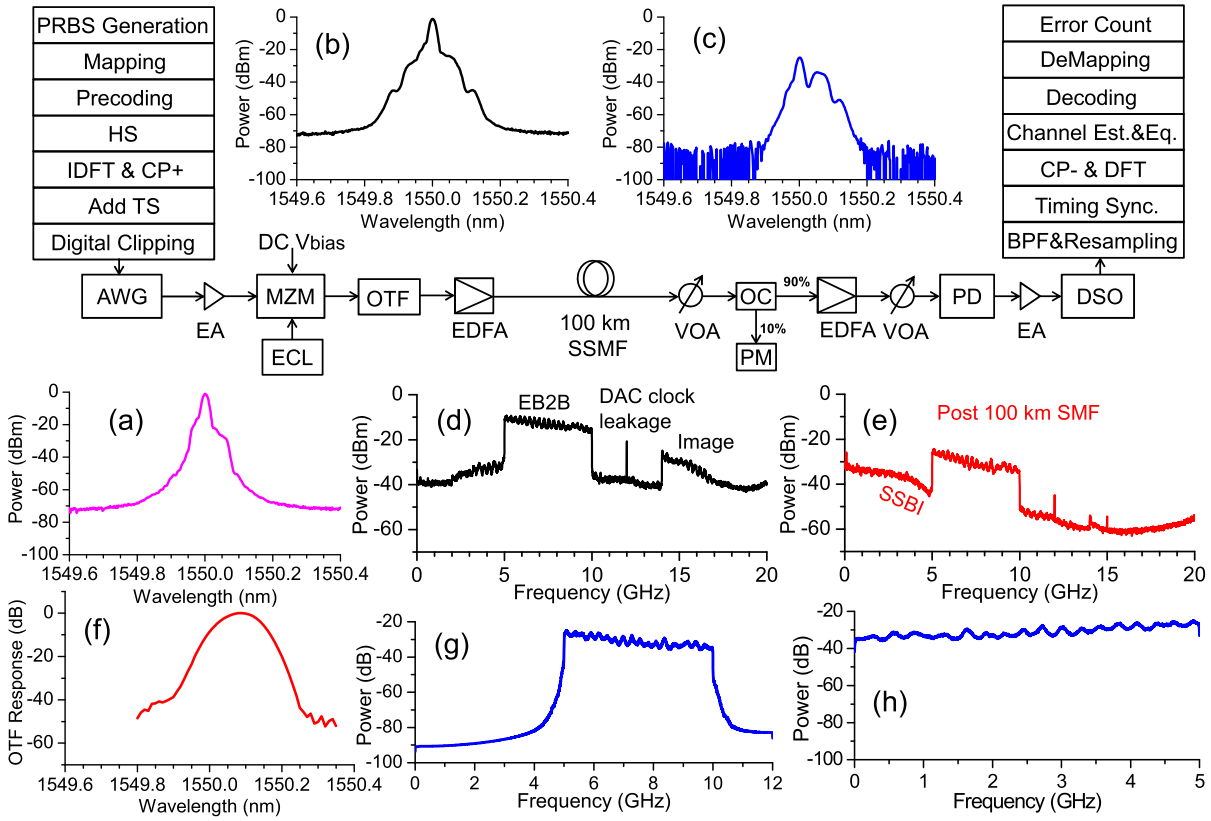

FIGURE 2. **Experimental setup of the GB-OSSB-OFDM transmission system and the corresponding optical/electrical spectra: (a) optical carrier; (b) GB-ODSB-OFDM; (c) GB-OSSB-OFDM; (d) the transmitted and (e) received samples at 40 GSa/s; (f) OTF response; (g) the down-sampled samples at 24 GSa/s; (h) the down-sampled samples at 10 GSa/s.**

also generated to obtain two types of training symbols (TS). One is used for timing synchronization with a single TS; the other is applied to realize channel estimation with 4 TSs. The IDFT size is 4800. The number of data subcarriers is 999, and the 2,000-th subcarrier is reserved and filled with zero. Other positive-frequency subcarriers are set to zeros for guard-band generation and oversampling. Before IDFT operation, the mapped data are optionally precoded with DFT and conjugate data on the negative-frequency bins are constructed to satisfy HS. The data after the insertions of CP and TSs are digitally clipped to further reduce PAPR and DAC quantitation noise. The clipping ratio (CR) in decibel is defined as $20\times \log_{10}(A/rms[x(n)])$, where $x(n)$ is the OFDM signal before digital clipping and A is the clipping threshold value; $rms[x(n)]$ is the root mean square value of $x(n)$. It should be noted that the clipping noise is small and can be ignored for the precoded signal at the CR of 11 dB. The key parameters for the GB-OFDM signal and experiment are listed in Table 1.

An OFDM frame consists of 5 TSs and 100 data-carrying GB-OFDM symbols are stored and uploaded to a Tektronix arbitrary waveform generator (AWG, AWG7122C) worked at 24 GSa/s. The converted signal is amplified by an electrical amplifier (EA). The electrical spectrum of the amplified signal is plotted in Fig. 2(d). It shows that there is a frequency component at 12 GHz due to DAC clock leakage. Meanwhile, the high-frequency spectral image is also observed, which is induced by the DAC's zero-order hold. The amplified signal directly drives a single-drive MZM. The optical source is an external cavity laser (ECL). An optical tunable filter (OTF) is employed to generate the guard-band OSSB signal. The lower sideband is suppressed by more than 20 dB. The optical spectra (0.02 nm resolution) of the ODSB and OSSB-OFDM signals are shown in Fig. 2(b) and 2(c), respectively. The OTF response is also plotted in Fig. 2(f). The CSPR of the OSSB signal is first reduced by the OTF and can be further adjusted by changing the DC bias voltage of MZM [25]. The CSPR of the OSSB signal as shown in Fig. 2(b) is 4 dB. The OSSB signal is boosted with an erbium-doped fiber amplifier (EDFA) and coupled to two spans of 50 km SSMF. The launch power is 8 dBm.

A variable optical attenuator (VOA) after a 100 km SSMF link is used to change the received optical power (ROP). With the help of an optical coupler (OC) in the ratio of 90:10, the ROP can be measured online with a power meter (PM) before an EDFA pre-amplifier. At the same time, the boosted signal is attenuated to -4 dBm and directly detected by a photodiode (PD). Subsequently, the received electrical signal is amplified and sampled by a Lecroy digital storage oscilloscope (DSO) operating at 40 GSa/s. Since there is not suitable

TABLE 1. Key parameters for the GB-OFDM signal and experiment.

Item	Parameter	Value
OFDM frame	IDFT/DFT size (N/2M)	4800/2000
	Data subcarriers (indices)	999 (1001-1999)
	Modulation format	16QAM
	CP length N_{CP}/N_{CPR}	24/10
	Digital CR	11 dB
AWG (DAC)	Sampling rate	24 GSa/s
	Vertical resolution	10 bits
EA	3dB Bandwidth	14 GHz
	Wavelength	1550 nm
ECL	Output power	14 dBm
	Linewidth	100 kHz
MZM	3 dB bandwidth	12 GHz
	Half-wave voltage	4.5 V
OTF	3 dB bandwidth	0.1 nm
	Central wavelength	1550.08 nm
EDFA	Noise figure	5 dB
SSMF	Length	100 km
	Attenuation	0.18 dB/km
	Dispersion	17 ns/nm/km
PD	3 dB bandwidth	10 GHz
DSO (ADC)	Sampling rate	40 GSa/s
	Vertical resolution	8 bits
	Bandwidth	20 GHz

electrical band-pass filter (BPF) in our lab, which is used to remove the SSBI occupying the guard band and avoid aliasing after undersampling. The results based on the proposed ADC undersampling are emulated with an offline DSP with digital BPF and resampling function. A similar emulation method can be found in [22], [24]. In our experiment, the bandwidth of the GB-OFDM signal is 5 GHz. Therefore, the filtered samples are down-sampled to 10 GSa/s for emulation of the ADC undersampling. For a comparison purpose, the 24 GSa/s samples are also obtained for conventional demodulation by down-sampling the filtered samples. The power spectra of the resampled samples at 24 GSa/s and 10 GSa/s are inserted in Fig. 2(g) and 2(h), respectively.

The receiver DSP algorithms include BPF and resampling, TS-based timing synchronization [28], CP removal, DFT, least square-based channel estimation with both inter-symbol frequency-domain averaging over 4 TSs and intra-symbol frequency averaging (ISFA) [29], [30], optional DFT decoding, zero-forcing based channel equalization, and demapping. The signal-to-noise ratio (SNR) is also estimated and the errors are directly counted over the data-carrying GB-OFDM symbols. According to the conclusion presented in [31], the SNR can be estimated by calculating the EVM of the recovered QAM symbols. The estimated SNR can be defined in decibel as

$$SNR_{dB} = -20\log_{10}\left(\sqrt{\frac{1}{N_s}\sum_{k=1}^{N_s}|e_k|^2 \Big/ \frac{1}{N_s}\sum_{k=1}^{N_s}|X_k|^2}\right) \quad (7)$$

where X_k denotes the reference QAM symbol, Y_k is recovered version, N_s is the number of the transmitted QAM symbols, and $e_k = Y_k - X_k$ is the error signal.

It should be noted that the same transmitter DSP algorithms are used in the conventional OFDM system and the system with the undersampling technique. The DSP flow in the receiver with undersampling is the same as the conventional one. However, the implementation complexity of the symbol timing synchronization and DFT operation for the undersampled OFDM is lower than that of the conventional OFDM. This fact is due to the reduced symbol length and DFT size after the proposed ADC undersampling.

V. EXPERIMENTAL RESULTS AND DISCUSSION

We investigate the PAPR performance of the baseband GB-OFDM signal by the means of numerical simulation. The CCDF is calculated over 50,000 OFDM symbols, as shown in Fig. 3. It can be seen clearly that the PAPR of the GB-OFDM signal can be obviously reduced by using DFT precoding technique. And about 6 and 7 dB PAPR reductions can be obtained at the CCDF of 1×10^{-3} and 1×10^{-4}, respectively, compared to the conventional GB-OFDM signal.

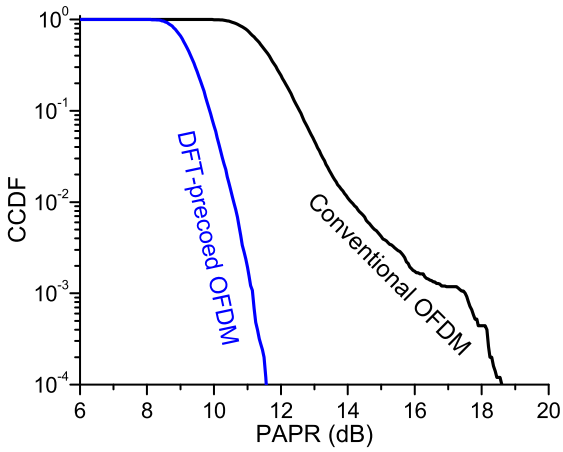

FIGURE 3. Simulated CCDFs of the guard-band OFDM signals.

Two different sampling rates of 24 GSa/s and 10 GSa/s are discussed for both EB2B and post-SSMF transmission cases. The estimated SNR of the guard-band signal with or without precoding as a function of the subcarrier (SC) index is shown in Fig. 4. It exhibits that the same SNR performance can be achieved by using the undersampling technique compared to the normal sampling case (24 GSa/s). In Fig. 4(a), the degraded SNR performance on the high-frequency SCs after 100 km SSMF transmission is mainly attributed to non-flat responses of MZM and PD. DFT-precoding can balance

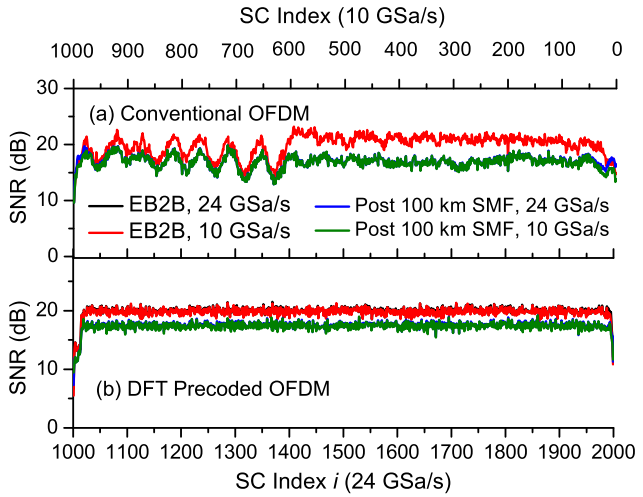

FIGURE 4. The estimated SNRs versus SC index: (a) conventional OFDM; (b) DFT precoded OFDM.

SNR over the data-carrying SCs. And the SNR balance can be obtained by using the DFT precoding technique. The bad SNR performance on the edge SCs is observed with the DFT precoding technique. This is due to inter-symbol interference (ISI). Nevertheless, the averaging SNR of DFT-precoded GB-OFDM is slightly higher than that of the conventional one. This benefit may come from its low PAPR.

The bit errors on each SC are counted after 100 km SSMF transmission with undersampling (10 GSa/s) and shown in Fig. 5. Even though more errors occur on the edge SCs with DFT precoding, the overall errors on the data-carrying SCs are less than that of the conventional one. The constellation diagrams of conventional and DFT precoded GB-OFDM are shown in Figs. 6(a-b) and the corresponding BER values are 1.3×10^{-3} and 7.3×10^{-4}, respectively. A longer CP can be applied to solve this problem and further improve BER performance by using the DFT precoding technique. The related results can be found in our previous work in [32].

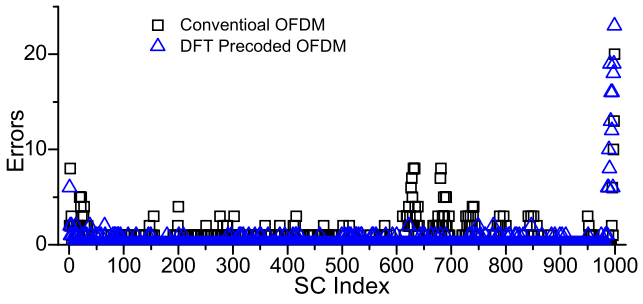

FIGURE 5. The measured bit errors versus SC index.

We change the DC bias voltage for the MZM to obtain the guard-band OSSB signals with CSPRs of 0, 2 and 4 dB. The measured BER performance as a function of ROP is presented in Fig. 7. It indicates that the DFT precoded GB-OFDM outperforms the conventional one in different CSPR cases. A similar BER performance can be achieved

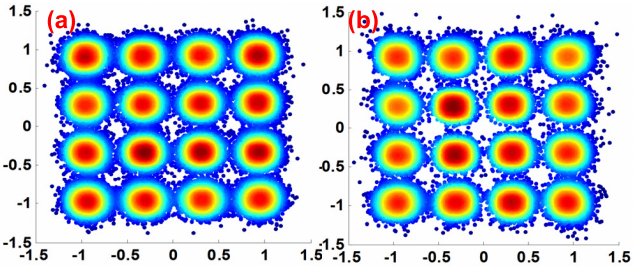

FIGURE 6. The recovered 16-QAM constellation diagrams: (a) conventional and (b) DFT-precoded GB-OFDM.

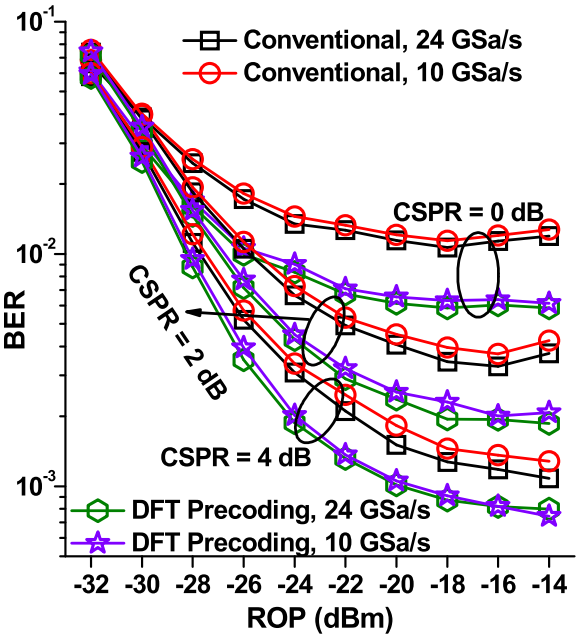

FIGURE 7. Offline measured BER performance versus ROP.

by the undersampling technique in comparison with the normal sampling one. The receiver sensitivity in terms of ROP at the optimal CSPR can be improved by about 2 dB by using DFT precoding techniques at the BER of 3.8×10^{-3}. Meanwhile, the required ROPs of the DFT-precoded systems with the BER of 3.8×10^{-3} are -23, -26 and -24.5 dBm when CSPRs are -2, -4 and -6 dB, respectively. Therefore, the optimal CSPR in our experiments is about 4 dB. This is mainly due to SSBI caused by DAC clock leakage and high-frequency spectral image as shown in Fig. 2 (d). In piratical applications, a low-pass filter can be used to suppress these two types of spectral interference.

VI. CONCLUSION

In this work, the DFT precoded GB-OSSB-OFDM signal reception with ADC undersampling technique was proposed and experimentally demonstrated for the first time. The PAPR of the GB-OFDM signal can be reduced significantly by up to 6 dB at the CCDF of 1×10^{-3} by using the DFT precoding technique. Moreover, there is a similar BER performance with the proposed ADC undersampling technique compared to conventional ADC oversampled GB-OFDM. At the optimal CSPR of 4 dB in our experiment, the receiver

sensitivity in terms of received optical power can be improved by 2 dB with the DFT precoding technique at the BER of 3.8×10^{-3}.

REFERENCES

[1] *IEEE P802.3bs 200 Gb/s and 400 Gb/s Ethernet Task Force*, IEEE Standard 802.3bs-2017. [Online]. Available: http://www.ieee802.org/3/bs/index.html
[2] N.-P. Diamantopoulos, K. Shikama, H. Nishi, T. Fujii, T. Kishi, K. Takeda, Y. Abe, T. Matsui, T. Kakitsuka, H. Fukuda, K. Nakajima, and S. Matsuo, "400-Gb/s DMT-SDM transmission based on membrane DML-array-on-silicon," *J. Lightw. Technol.*, vol. 37, no. 8, pp. 1805–1812, Apr. 15, 2019.
[3] T. Chan, I.-C. Lu, J. Chen, and W. I. Way, "400-Gb/s transmission over 10-km SSMF using discrete multitone and 1.3-μm EMLs," *IEEE Photon. Technol. Lett.*, vol. 26, no. 16, pp. 1657–1660, Aug. 15, 2014.
[4] *ITU-T 40-Gigabit-Capable Passive Optical Networks (NG-PON2): General Requirements*, document ITU-T G.989.1. [Online]. Available: https://www.itu.int/rec/T-REC-G.989.1/en
[5] B. J. C. Schmidt, A. J. Lowery, and J. Armstrong, "Experimental demonstrations of electronic dispersion compensation for long-haul transmission using direct-detection optical OFDM," *J. Lightw. Technol.*, vol. 26, no. 1, pp. 196–203, Jan. 1, 2008.
[6] X. Xiao, F. Li, J. Yu, Y. Xia, and Y. Chen, "Real-time demonstration of 100Gbps class dual-carrier DDO-16QAM-DMT transmission with directly modulated laser," in *Proc. Opt. Fiber Commun. Conf.*, 2014, Paper M2E.6.
[7] R. Bouziane, P. A. Milder, S. Erkilinç, L. Galdino, S. Kilmurray, B. C. Thomsen, P. Bayvel, and R. I. Killey, "Experimental demonstration of 30 Gb/s direct-detection optical OFDM transmission with blind symbol synchronisation using virtual subcarriers," *Opt. Express*, vol. 22, no. 4, pp. 4342–4348, Feb. 2014.
[8] D. Qian, N. Cvijetic, J. Hu, and T. Wang, "108 Gb/s OFDMA-PON with polarization multiplexing and direct detection," *J. Lightw. Technol.*, vol. 28, no. 4, pp. 484–493, Feb. 15, 2010.
[9] N. Cvijetic, M.-F. Huang, E. Ip, Y. Shao, Y.-K. Huang, M. Cvijetic, and T. Wang, "Coherent 40Gb/s OFDMA-PON for long-reach (100^{+}km) high-split ratio (>1:64) optical access/metro networks," in *Proc. OFC*, 2012, Paper. OW4B.8.
[10] Q. Yang, W. Shieh, and I. B. Djordjevic, "1-Tb/s large girth LDPC-coded coherent optical OFDM transmission over 1040-km standard single-mode fiber," in *Proc. Opt. Fiber Commun. Conf./Nat. Fiber Opt. Eng. Conf.*, 2011, Paper ThA35.
[11] Y. Xu, M. Lyu, L. Rusch, and W. Shi, "Silicon microring IQ modulator enabled single sideband OFDM transmission," in *Proc. Opt. Fiber Commun. Conf. (OFC)*, 2019, Paper Th2A.28.
[12] A. Ali, J. Leibrich, and W. Rosenkranz, "Spectral efficiency and receiver sensitivity in direct detection optical-OFDM," in *Proc. Opt. Fiber Commun. Conf. Nat. Fiber Opt. Eng. Conf.*, 2009, Paper OMT7.
[13] W.-R. Peng, X. Wu, V. Arbab, K.-M. Feng, B. Shamee, L. Christen, J.-Y. Yang, A. Willner, and S. Chi, "Theoretical and experimental investigations of direct-detected RF-tone-assisted optical OFDM systems," *J. Lightw. Technol.*, vol. 27, no. 10, pp. 1332–1339, May 15, 2009.
[14] J. Ma, "Influence of the device parameters in ICRBD on SSB-OOFDM signal with reduced guard band," *Opt. Express*, vol. 22, no. 24, p. 29636, Dec. 2014.
[15] S. You, Y. Wang, W. Liu, Y. Shen, J. Pang, X. Li, and M. Luo, "400-Gb/s single-sideband direct detection over 7-core fiber with SSBI cancellation," *IEEE Photon. Technol. Lett.*, vol. 31, no. 9, pp. 669–672, May 1, 2019.
[16] W.-R. Peng, X. Wu, K.-M. Feng, V. R. Arbab, B. Shamee, J.-Y. Yang, L. C. Christen, A. E. Willner, and S. Chi, "Spectrally efficient direct-detected OFDM transmission employing an iterative estimation and cancellation technique," *Opt. Express*, vol. 17, no. 11, pp. 9099–9111, May 2009.
[17] T. Bo and H. Kim, "Kramers-Kronig receiver operable without digital upsampling," *Opt. Express*, vol. 26, no. 11, pp. 13810–13818, May 2018.
[18] L. Zhang, T. Zuo, Q. Zhang, J. Zhou, E. Zhou, and G. N. Liu, "150-Gb/s DMT over 80-km SMF transmission based on spectrally efficient SSBI cancellation using guard-band twin-SSB technique," in *Proc. ECOC*, 2016, pp. 1178–1180.
[19] M. Chen, M. Peng, H. Zhou, Z. Zheng, X. Tang, and L. Maivan, "Receiver sensitivity improvement in spectrally-efficient guard-band twin-SSB-OFDM using an optical IQ modulator," *Opt. Commun.*, vol. 405, pp. 259–264, Dec. 2017.
[20] H.-C. Liu, C.-H. Lin, C.-T. Lin, C.-C. Wei, H.-T. Huang, H.-H. Hsu, M.-F. Wu, and S. Chi, "Simple receiving scheme in 100-GHz DD OFDM RoF systems employing low-sampling-rate ADCs and digital preprocess," in *Proc. Opt. Fiber Commun. Conf.*, 2015, Paper Th2A.7.
[21] L. Cheng, X. Liu, N. Chard, F. Effenberger, and G.-K. Chang, "Experimental demonstration of sub-Nyquist sampling for bandwidth- and hardware-efficient mobile fronthaul supporting 128×128 MIMO with 100-MHz OFDM signals," in *Proc. Opt. Fiber Commun. Conf.*, 2016, Paper W3C.3.
[22] L. Cheng, H. Wen, X. Zheng, H. Zhang, and B. Zhou, "Channel characteristic division OFDM-PON for next generation optical access," *Opt. Exp.*, vol. 19, no. 20, pp. 19129–19134, Sep. 2011.
[23] C.-C. Wei, H.-C. Liu, C.-T. Lin, and S. Chi, "Analog-to-digital conversion using sub-Nyquist sampling rate in flexible delay-division multiplexing OFDMA PONs," *J. Lightw. Technol.*, vol. 34, no. 10, pp. 2381–2390, May 15, 2016.
[24] J.-H. Hsu, M. Yu, F. Liu, C.-H. Lin, C.-T. Lin, L. Zhou, L. Fang, and C.-C. Wei, "On channel estimation schemes for APD-based DDM-OFDM-PONs under sub-Nyquist sampling," *Opt. Express*, vol. 26, no. 18, pp. 23808–23818, Sep. 2018.
[25] M. Chen, Q. Chen, H. Zhou, Z. Zheng, J. He, and L. Chen, "Low-complexity receiver using undersampling for guard-band SSB-DDO-OFDM," *IEEE Photon. J.*, vol. 9, no. 4, pp. 1–12, Aug. 2017.
[26] A. Tolmachev, M. Orbach, M. Meltsin, R. Hilgendorf, Y. Birk, and M. Nazarathy, "Real-time FPGA implementation of efficient filter-banks for digitally sub-banded coherent DFT-S OFDM receiver," in *Proc. Opt. Fiber Commun. Conf./Nat. Fiber Opt. Eng. Conf.*, 2013, paper OW3B.1.
[27] F. Li, J. Yu, Y. Fang, Z. Dong, X. Li, and L. Chen, "Demonstration of DFT-spread 256QAM-OFDM signal transmission with cost-effective directly modulated laser," *Opt. Express*, vol. 22, no. 7, pp. 8742–8748, Apr. 2014.
[28] M. Chen, J. He, Q. Fan, Z. Dong, and L. Chen, "Experimental demonstration of real-time high-level QAM-encoded direct-detection optical OFDM systems," *J. Lightw. Technol.*, vol. 33, no. 22, pp. 4632–4639, Nov. 15, 2015.
[29] X. Liu and F. Buchali, "Intra-symbol frequency-domain averaging based channel estimation for coherent optical OFDM," *Opt. Express*, vol. 16, no. 26, p. 21944–21957, Dec. 2008.
[30] Q. Yang, N. Kaneda, X. Liu, and W. Shieh, "Demonstration of frequency-domain averaging based channel estimation for 40-Gb/s CO-OFDM with high PMD," *IEEE Photon. Technol. Lett.*, vol. 21, no. 20, pp. 1544–1546, Oct. 15, 2009.
[31] R. A. Shafik, M. S. Rahman, and A. R. Islam, "On the extended relationships among EVM, BER and SNR as performance metrics," in *Proc. Int. Conf. Electr. Comput. Eng.*, Dec. 2006, pp. 408–411.
[32] M. Chen, X. Xiao, Z. R. Huang, J. Yu, F. Li, Q. Chen, and L. Chen, "Experimental demonstration of an IFFT/FFT size efficient DFT-spread OFDM for short reach optical transmission systems," *J. Lightw. Technol.*, vol. 34, no. 9, pp. 2100–2105, May 1, 2016.

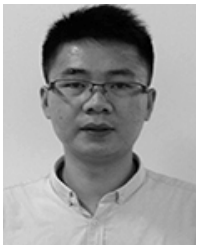

MING CHEN (Member, IEEE) received the Ph.D. degree from Hunan University, Changsha, China, in 2015. He was a Visiting Scholar with the Rensselaer Polytechnic Institute, NY, USA, in 2016. He is currently an Associate Professor with the School of Physics and Electronics, Hunan Normal University. He has authored or coauthored over 70 reviewed journal and conference proceeding articles. His research interests include advanced modulation formats, radio over fiber, real-time digital signal processing, and optical communications.

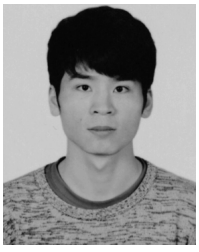

LONG ZHANG received the bachelor's degree in applied physics from the Southwest University of Science and Technology, China, in 2017. He is currently pursuing the master's degree with Hunan Normal University. His research interests include optical fiber communication, channel estimation, and advanced modulation formats.

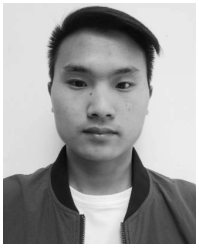

DONGSHENG XI received the bachelor's degree in physics from Pingdingshan University, China, in 2018. He is currently pursuing the master's degree with Hunan Normal University. His research interests include optical fiber communication and optical orthogonal frequency-division multiplexing.

GANG LIU received the bachelor's degree in electronic science and technology from Shaoyang University, China, in 2017. He is currently pursuing the master's degree with Hunan Normal University. His research interests include optical fiber communication and precoding technique.

HUI ZHOU received the B.S. degree from the National University of Defense Technology, Changsha, China, in 2007, and the M.S. and Ph.D. degrees from Hunan University, Changsha, in 2010 and 2014, respectively. From 2018 to 2019, she was an Academic Scholar with Fudan University, Shanghai, China. She is currently a Lecturer with Hunan Normal University. Her current research interests include nonlinear optics, optical orthogonal frequency division multiplexing communication, and radio-over-fiber systems.

QINGHUI CHEN received the bachelor's degree in computer science and technology from Nanhua University, China, in 2003, and the M.Sc. and Ph.D. degrees from Hunan University, China, in 2010 and 2018, respectively. She is currently a Senior Engineer with the College of Computer Science, Hunan University of Technology. Her research interests include modulation format, optical signal processing, visible light communication, and optical camera communication.